

Silica Nanoparticles Modified with Trithiocyanuric Acid as a Potential Adsorbent for Removal of Ag^+ from Aqueous Solutions

Likang Fu · Libo Zhang · Shixing Wang ·
Jinhui Peng · Gengwei Zhang

Received: 19 December 2016 / Accepted: 29 June 2017 / Published online: 11 July 2017
© Springer International Publishing AG 2017

Abstract Surface modification of the silica nanoparticles was performed using trithiocyanuric acid (TCA-SNPs) so as to enhance the adsorption of Ag^+ from aqueous solutions. The surface modification to the adsorbent was characterized by Fourier transform infrared spectroscopy, transmission electron microscope, and X-ray photoelectron spectroscopy. The Ag^+ adsorption capacity was found to increase with increase in the solution pH, with the optimal pH being 5.0. The Ag^+ adsorption isotherm was generated at 25 °C at the optimal solution pH and the maximum adsorption capacity was found to be 80 mg/g, significantly higher than the adsorption capacity reported for other adsorbents in literature. The increase in adsorption capacity was attributed to the presence of thiol groups on the surface of the modified adsorbents. Additionally, the adsorption kinetics was estimated at 25 °C, which indicated very high rates of adsorption initially, with rapid reduction in rate of adsorption with time. Both adsorption isotherms as well as the adsorption kinetics were modeled with

popular models. The adsorption isotherm was found to match with the Langmuir model while the adsorption kinetics was found to match with the pseudo-second-order kinetic model. The adsorption-desorption cycles indicate the TCA-SNPs to be stable adsorption performance and retain high adsorption efficiency ensuring commercial adoption. A relatively low adsorption of other ions such as Mn^{2+} , Cu^{2+} , Ni^{2+} , Co^{3+} as compared to Ag^+ was ensured.

Keywords Silica nanoparticles · Trithiocyanuric acid · Adsorption · Silver ions

1 Introduction

Silver plays an essential role in various industries which include photography, electroplating, medical science, rechargeable battery, and metal alloys (Pourreza et al. 2014; Zeliyha et al. 2010). However, recent reports evidence release of thousands tons of silver annually into waste water streams (Eckelman and Graedel 2007; Peng et al. 2015). Such a widespread, large-scale discharges of the monovalent ionic silver, Ag^+ , can lead to assimilation and accumulation which living organisms exposed to it. Exposure to Ag^+ is well known to be of high level toxicity, possibly causing various disorders and diseases, such as hypertension, behavioral changes, and oxidative stress (Chang et al. 2006; Monier et al. 2010; Hassan and El-Wakil 2003; Shin et al. 2011; Bose et al. 2002; Cecen et al. 2010). Hence, it is mandatory to

L. Fu · L. Zhang · S. Wang · J. Peng · G. Zhang
State Key Laboratory of Complex Nonferrous Metal Resources
Clean Utilization, Kunming 650093, China

L. Fu · L. Zhang · S. Wang · J. Peng · G. Zhang
National Local Joint Laboratory of Engineering Application of
Microwave Energy and Equipment Technology,
Kunming 650093, China

L. Fu · L. Zhang · S. Wang (✉) · J. Peng · G. Zhang
Faculty of Metallurgical and Energy Engineering, Kunming
University of Science and Technology, Kunming 650093, China
e-mail: wsxkm@sina.com

remove Ag^+ from water streams to the permissible discharge limits.

A thorough review of literature reveal various methods for treatment/removal of Ag^+ from industrial waste water, which include liquid-liquid extraction (EI-Shahawi et al. 2007), cloud point extraction (Ghaedi et al. 2009; Manzoori et al. 2007), ion-exchange, adsorption method (Moshhadizadeh and Karami 2011; Tahmasebi and Yamini 2014), and membrane technique (Soylak and Cay 2007; Tang et al. 2010). Among the aforementioned separation technology, adsorption is reported to be most promising due to easy operation, higher adsorption capacity, and economical. Among the various adsorbents, nano-adsorbents have received recent research focus due to their better physiochemical properties for removal of pollutants from waste water (Nguyen-Phan et al. 2010; Zhang et al. 2013). Application of silica nanoparticle is reported for removal of various heavy metal ions (Pourreza et al. 2014; Zhang et al. 2016), copper (Ali et al. 2016), mercury (He et al. 2015), lead (Li et al. 2015), uranium (Zhao et al. 2014a, b, 2015), cadmium, and nickel (Xie et al. 2008).

The present work attempts to modify the surface chemistry of the silica nanoparticles through incorporation of nitrogen groups on the surface. The silica nanoparticles are naturally hydrophilic owing to the presence of OH groups on the surface thus restricting its application to liquid phase adsorption. Additionally, the presences of oxygen functional groups render it acidic in nature. Hence, an attempt to modify the surface with replacement of OH group to render it hydrophobic as well as to increase the basicity of the adsorbent through incorporation of nitrogen and thiol groups. Towards which trithiocyanuric acid was utilized to modify the surface of silica nanoparticles. The surface modified silica nanoparticles were characterized by Fourier transform infrared spectroscopy (FT-IR), X-ray photoelectron spectroscopy (XPS), and transmission electron microscope (TEM). The surface-modified silica nanoparticles were utilized to remove the Ag^+ from liquid phase through a systematic study assessing the effects of pH, developing adsorption isotherm of Ag^+ , and kinetics of adsorption. The adsorption isotherms as well as the kinetics

of adsorption were modeled utilizing well-known models.

2 Materials and Methods

2.1 Materials

Silica nanoparticles (SNPs, Hydrophilic-380, 99.8%), trithiocyanuric acid (TCA, 98%), 3-glycidyloxypropyltrimethoxysilane (GPTMS, 98%), cyanuric chloride (CC, 99%), and polyethyleneimine (PEI, M.W.600, 99%) were purchased from Aladdin Chemistry Co. Ltd. Potassium iodide (99%), AgNO_3 (99.7%), $\text{Mn}(\text{NO}_3)_2$ (99.5%), $\text{Ni}(\text{NO}_3)_2$ (99.5%), $\text{Cu}(\text{NO}_3)_2$ (99.5%), $\text{Co}(\text{NO}_3)_3$ (99.5%), triethylamine (99.5%), tetrahydrofuran (THF, 99.5%), methanol (99.7%), ethanol (99.8%), thiourea (99%), NaOH (99%), and HNO_3 (99.5%) were purchased from Tianjin Chemical Reagent Co. Ltd.

2.2 Function of Silica Nanoparticles with Trithiocyanuric Acid

The surface modification procedure of SNPs with trithiocyanuric acid is presented in Fig. 1. Firstly, epoxy group was grafted on the surface of SNPs via silanation process. Five grams (0.083 mol) of SNPs along with 10 g of GPTMS (0.042 mol) and 50 mL of ethanol were added into a 100-mL three-necked flask. The mixture was stirred and refluxed for 24 h. After the suspension was centrifuged for 5 min by high speed centrifuge (10,000 rpm), the precipitate was washed with ethanol repeatedly for five times and dried at 60 °C overnight and sample named as GPTMS-SNPs. Secondly, PEI-functionalization was carried out by ring-opening reaction between the epoxy groups and the amine groups. Towards which 4.40 g (0.014 mol) of GPTMS-SNPs was stirred in 40 mL of ethanol solution containing 0.17 mol /L of PEI at 70 °C for 24 h. Then the mixture was centrifuged for 5 min by high speed centrifuge (10,000 rpm), to separate the precipitate which was washed with deionized water for five times and dried at 60 °C for 12 h. This sample is denoted as PEI-SNPs. Subsequent modification step was conducted by reacting PEI-SNPs with cyanuric chloride. Towards which

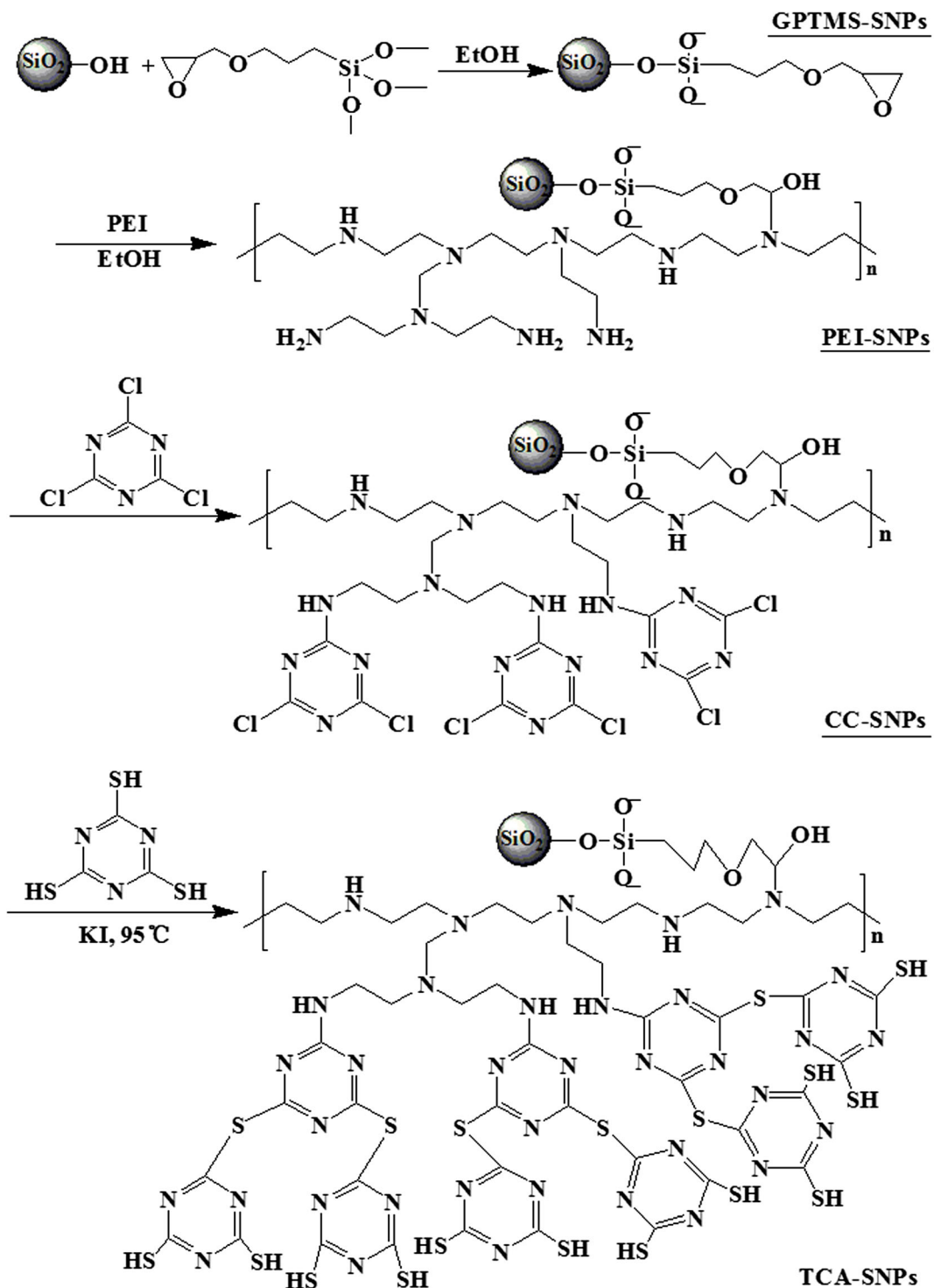


Fig. 1 The modification process of silica nanoparticles

0.46 g (0.003 mol) of cyanuric chloride and 5.98 mL of triethylamine were dissolved in

100 mL of dried tetrahydrofuran (THF), and 3.50 g (0.587 mmol) of PEI-SNPs. The mixture

was refluxed for 24 h, and then was centrifuged for 5 min by high speed centrifuge (10,000 rpm). The solid was washed with THF for five times, dried at 60 °C for 12 h and sample identified as CC-SNPs. Lastly, CC-SNPs were functionalized with trithiocyanuric acid. Towards which trithiocyanuric acid of 2.30 g (0.013 mol) and 3.00 g (0.404 mmol) of CC-SNPs were added into a 250-mL three-necked flask and 1.62 g (0.010 mol) of potassium iodide was added as a catalyst, along with 50 mL of methanol and 30 mL of triethylamine. The mixture was refluxed at 95 °C for 24 h and then was centrifuged for 5 min by high speed centrifuge (10,000 rpm), washed with methanol five times, dried at 70 °C for 24 h, and denoted as TCA-SNPs.

2.3 Characterization

FT-IR was carried out using the infrared spectrophotometer (Thermo Nicolet, USA) in the range from 4000 to 400 cm^{-1} with solution of 1 cm^{-1} by KBr pellets. XPS was conducted with a PHI5000 Versaprobe-II (Physical Electronics, Inc., Chanhassen, MN, USA) using 200 W Mg-radiations. The suspension was centrifuged by high speed centrifuge (GT10-1, China). The size and morphology of silica nanoparticles were characterized by TEM (JEM-3200). The concentrations of Ag^+ , Mn^{2+} , Cu^{2+} , Ni^{2+} , and Co^{3+} were determined with Prodigy 7 (Leeman, USA) inductively coupled plasma optical emission spectrometer with an axial plasma viewing. Operating conditions for this spectrometer were as follows: RF power 1.10 kW, coolant flow 15 L/min, auxiliary flow 1.0 L/min, nebulizer pressure 1.0 L/min, uptake rate 25 rpm. The detection limit of ICP-OES is 0.2 ppm. The device of pH is PHS-3C pH meter (Rex, China). The image analysis software is DigitalMicrograph365 Demo.

2.4 Batch Adsorption Experiments

The adsorption of Ag^+ by TCA-SNPs was carried out in batch operation at pH 5.0 and 25 °C. Twenty milligrams of TCA-SNPs was suspended in 10 mL of the monovalent ionic silver solution in a shaker bath at 300 rpm for the duration of 5 h. The suspension was centrifuged at

10,000 rpm for 3 min. The residual concentration of Ag^+ in the supernatant solution was determined by ICP-OES. The removal percent (R , %) and equilibrium adsorption capacity (q , mg/g) of Ag^+ by TCA-SNPs were calculated according to the following Eq. (1) and Eq. (2):

$$R = \frac{(C_0 - C_e)}{C_0} \times 100\% \quad (1)$$

$$q = \frac{(C_0 - C_e)}{m} V \quad (2)$$

Where C_0 (mg/L) and C_e (mg/L) are the initial and final concentration of Ag^+ solution, respectively. V (L) is the volume of the monovalent ionic silver solution and m (mg) is the weight of adsorbent (TCA-SNPs). All the adsorption experiments were performed at least three times.

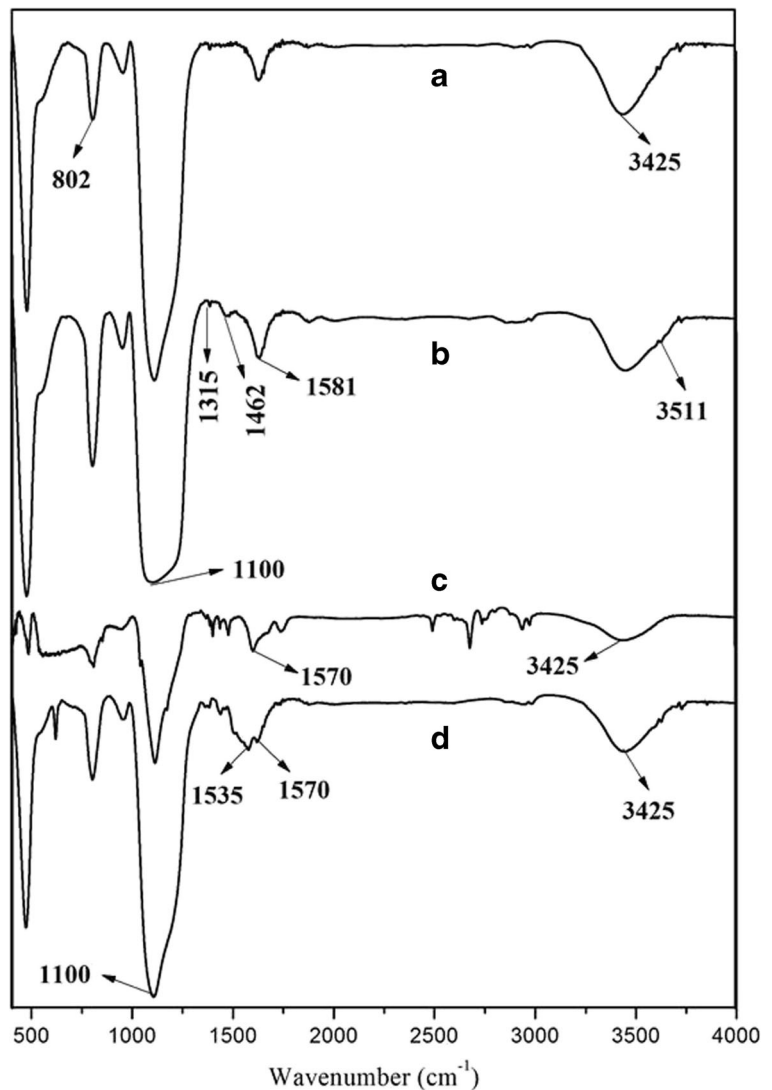
Twenty milligrams of TCA-SNPs was also added into 10 mL of solutions containing Ag^+ (100 mg/L) and coexisting ions (25 mg/L), such as Mn^{2+} , Cu^{2+} , Ni^{2+} , and Co^{3+} , and then oscillated it for 5 h at pH 5 and room temperature. After centrifuged and filtrated, we obtained the coexisting ions concentration from the supernatant.

3 Results and Discussion

3.1 Characterization of Absorbents

FT-IR techniques provide better observation and interpretation of subtle changes taking place during modifying of SNPs. Figure 2 shows the FT-IR spectra of the synthesized silica nanoparticles. The adsorption peaks at 3425 and 1100 cm^{-1} were attributed to the O-H and Si-O-Si stretching vibrations and the band at 802 cm^{-1} was assigned to the epoxy group (C-O-C) (Fig. 2(a)). After modified by PEI, the peaks at 1581, 1462, and 1315 cm^{-1} were ascribed to the $-\text{NH}_2$ and C-N stretching vibrations (Fig. 2(b)). The FT-IR spectra of CC-SNPs presented the N-H deformation vibrations at 1570 cm^{-1} and cyanuric ring vibrations at 1535 cm^{-1} (Fig. 2(c)). As shown in Fig. 2(d), the intensity of peaks at 1570 and 1535 cm^{-1} markedly increased after grafted trithiocyanuric acid.

Fig. 2 FT-IR spectra of GPTMS-SNPs (a), PEI-SNPs (b), CC-SNPs (c), and TCA-SNPs (d)



XPS is one of the most powerful tools for understanding the chemical composition and electronic structure analysis of a material. Figure 3 shows the characteristic peaks of *C1s*. The *C1s* of GPTMS-SNPs can be divided into two different peaks at 284.6 and 285.4 eV, belonging to the C-C and C-O species (Fig. 3a). After modified by PEI, the *C1s* of PEI-SNPs can be further divided into three different peaks at 284.6, 285.4, and 286.1 eV, attributing to the C-C, C-O, and C-N species, respectively (Fig. 3b). Figure 3c shows that the intensity of the *C1s* peaks at 287 eV increased after grafted the cyanuric chloride, belonging to the C-Cl group. The *C1s* of TCA-SNPs consisted of four peaks at 284.6, 285.4, 286.1, and 287.6 eV, corresponding to C-C, C-O, C-N, and C-S species, respectively (Fig. 3d). The results

indicate that the TCA-SNPs adsorbent had been successfully synthesized.

TEM is often used to observe the morphology or dispersion of the nanoparticles and to evaluate the size of the nanoparticles. As shown in Fig. 4, the particles size of SNPs and TCA-SNPs distribution calculated with image analysis software (DigitalMicrograph365 Demo) is both 13.5 ± 5.0 nm. The TEM images show that there is no noticeable difference in morphology and size between SNPs and TCA-SNPs.

3.2 Effect of pH

Owing to facilitate the dissociation of functional groups of adsorbent and influence the electrostatic adherence or

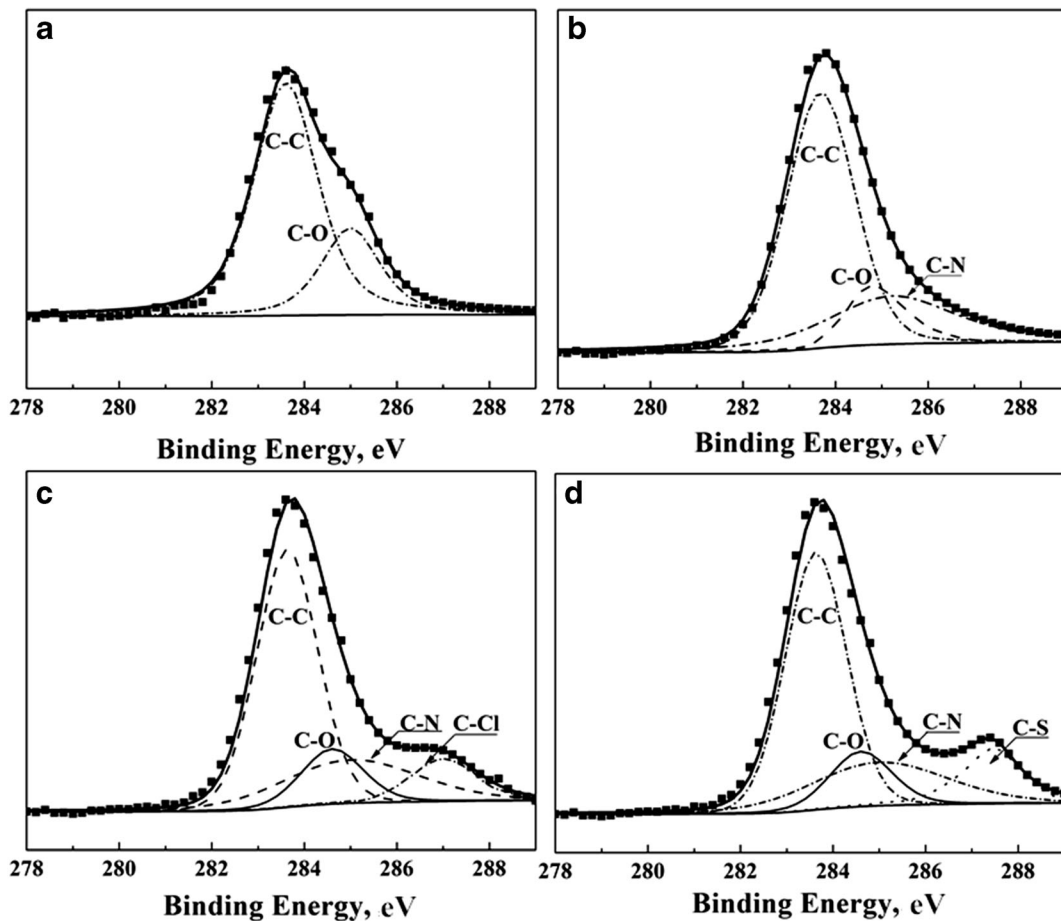
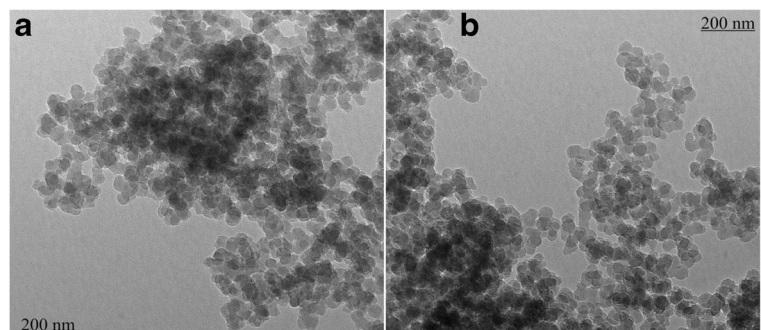


Fig. 3 C_{1s} of GPTMS-SNPs (a), PEI-SNPs (b), CC-SNPs (c), and TCA-SNPs (d)

complexation reactions at the adsorptive surface, it is a conventional practice to identify the optimum solution pH that would facilitate better adsorption of heavy metal ions (Pourreza et al. 2014; Manzoori et al. 2009). The effect of pH on Ag^+ adsorption was assessed within the pH range from 0.5 to 6.0. Since silver ion begins to precipitate as silver hydroxide when pH higher than 6.0, the range was restricted below a pH of 6.0. Twenty

milligrams of TCA-SNPs was added into 10 mL of the silver solution (100 mg/L) and oscillated for 5 h at room temperature. After centrifuged, we got the Ag^+ concentration from supernatant. Figure 5 shows that the adsorption capacity increase with an increase in solution pH, with the optimal pH being 5.0. The maximum adsorption capacity of Ag^+ on TCA-SNPs is found to be 80 mg/g. This could be explained that most of the

Fig. 4 TEM images of SNPs (a) and TCA-SNPs (b)



amine groups on the TCA-SNPs surface were protonated at low pH, which electrostatically repulsed silver ions (Hou et al. 2015), and the higher concentration of H_3O^+ ions at low pH will exhibit competitive complexation with Ag^+ (Lihareva et al. 2010).

3.3 Adsorption Isotherms

The adsorption isotherm at 25 °C was generated by varying the initial concentration of Ag^+ at a pH of 5.0, by adding the 20 mg of TCA-SNPs and reacting for 5 h. Figure 6 shows an increase in the adsorption capacity with increase in the initial concentration of Ag^+ , with the maximum adsorption capacity of about 80 mg/g. But the adsorption capacity of SNPs was only 7.5 mg/g. The adsorption capacity of TCA-SNPs, along with the literature-reported adsorption capacity for other adsorbents is listed in Table 1. The high adsorption capacity TCA-SNPs as compared to other adsorbents reported in literature could be attributed to the favorable presence of thiol groups on the surface of silica nanoparticles.

The experimental equilibrium data of Ag^+ on TCA-SNPs at pH 5.0 and 298 K were tested with various adsorption isotherm models such as Freundlich, Langmuir, Temkin, and Dubinin-Radushkevich models, to identify the suitable isotherm model. The model equations are reported in all the standard text books dealing with adsorption process and very widely in literature (Soumya et al. 2017, Saif et al. 2017, Reddy et al. 2016). It is a general practice to identify the suitable model through the goodness of fit and regression coefficient (R^2). Figure 7 shows the fit of the model along with the estimated model parameters for all the four models stated above. Table 2

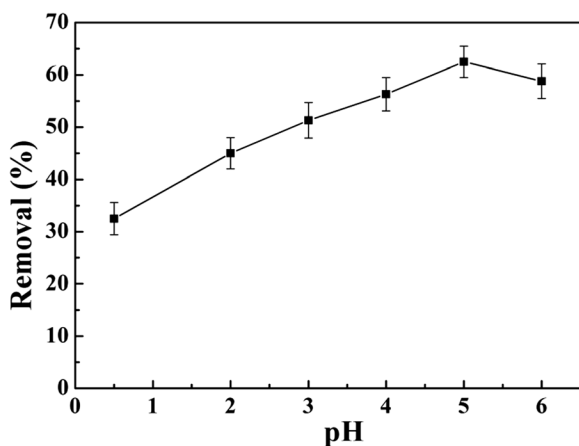


Fig. 5 Effect of pH on the adsorption of Ag^+

Table 1 Comparison of adsorption capacity of Ag^+ with adsorbents reported in literature

Adsorbent	q_m (mg/g)	Reference
SE-SNPs	21.90	Zhang et al. (2017)
Natural clinoptilolites	31.44	Coruh et al. (2010)
CNC _{SL}	56	Liu et al. (2015)
Thiourea-formaldehyde chelating resins	58.14	Kirci et al. (2009)
MFT chelating resin	60.05	Yirikoglu and GÜlfen (2008)
SNPs	7.5	This work
TCA-SNPs	80	This work

compiles the model parameters along with the R^2 value. Based on comparison of the R^2 value, it can be surmised that the Langmuir isotherm is the best followed by the Dubinin-Radushkevich model. The appropriate model isotherms along with suitable kinetics play an important role in the design of commercial adsorption columns.

3.4 Adsorption Kinetics

As stated earlier, adsorption isotherm along with adsorption kinetics play a major role in the design of adsorption columns. Hence, it is imperative to establish the adsorption kinetics and to model it with suitable kinetic model. The adsorption kinetic experiments were performed by adding 20 mg of TCA-SNPs to 100 mL Ag^+ solutions at pH = 5.0. Figure 8 shows the decrease in concentration of the Ag^+ ion in the solution with increase in contact time indicating the transfer to the

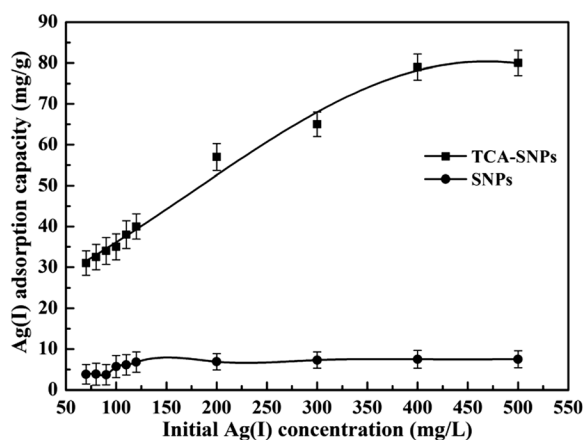


Fig. 6 Effect of initial Ag^+ concentration on Ag(I) adsorption

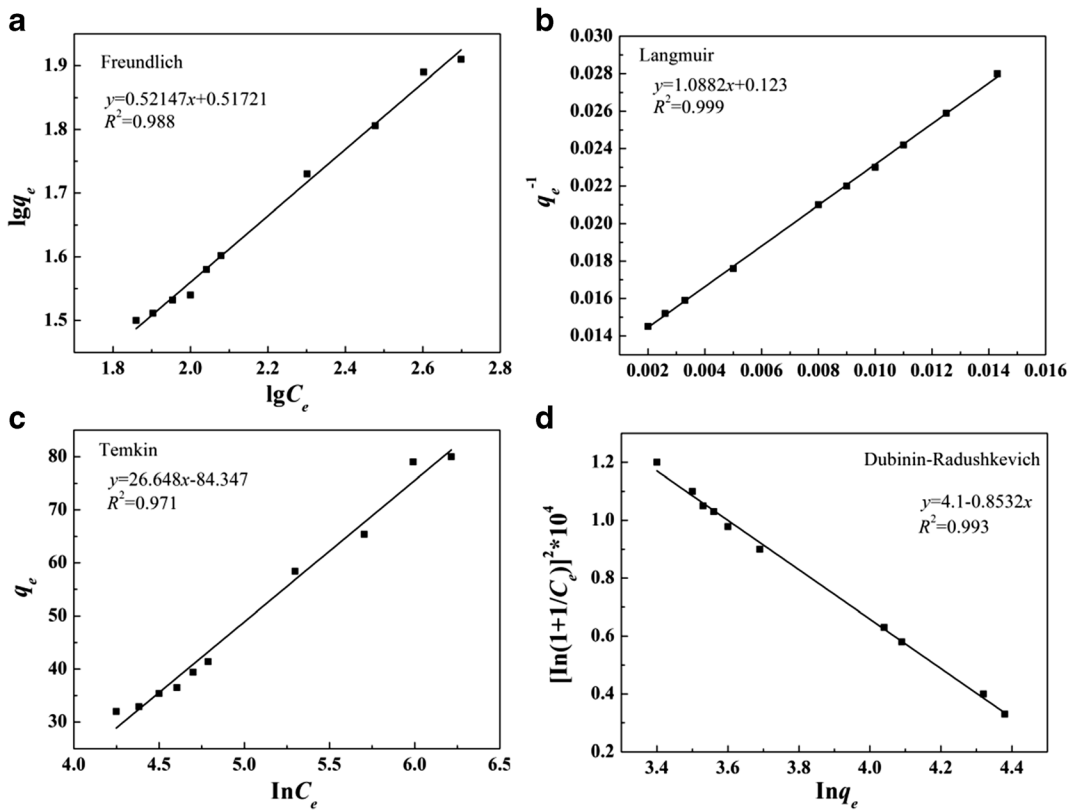


Fig. 7 Adsorption isotherm of Ag^+ adsorption on TCA-SNPs Freundlich (a), Langmuir (b), Temkin (c), and Dubinin-Radushkevich (d)

adsorbents phase. The rate of adsorption is fast until a contact time of 30 min beyond which significant change in the concentrations was not observed.

The rate of adsorption is modeled using the popular literature-reported kinetics models such as pseudo-first-order, pseudo-second-order, and intraparticle diffusion model. The kinetic model equations are very widely reported in literature and can also be sourced from

Table 2 Isotherm parameters for Ag^+ adsorption on TCA-SNPs at 298 K

Isotherm model	Parameter	Value
Freundlich	K_F $[(\text{mg g}^{-1})/(\text{mg L}^{-1})^{1/n}]$	3.2901
	n	1.9177
	R^2	0.988
Langmuir	q_m (mg/g)	81.30
	K_L (L/g)	7.4711
	R^2	0.999
Temkin	K_T (L/g)	0.4037
	b (J/mol)	92.974
	R^2	0.971
Dubinin-Radushkevich	q_m (mg/g)	60.34
	β ($\text{mol}^2 \text{kJ}^{-2}$)	1.41×10^{-7}
	R^2	0.993

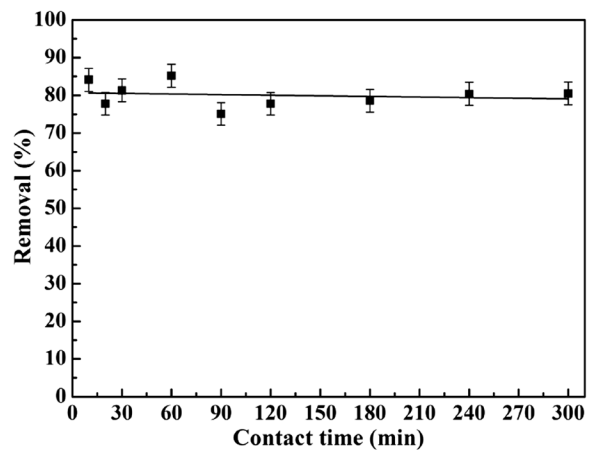


Fig. 8 Effect of contact time on Ag^+ adsorption onto the TCA-SNPs

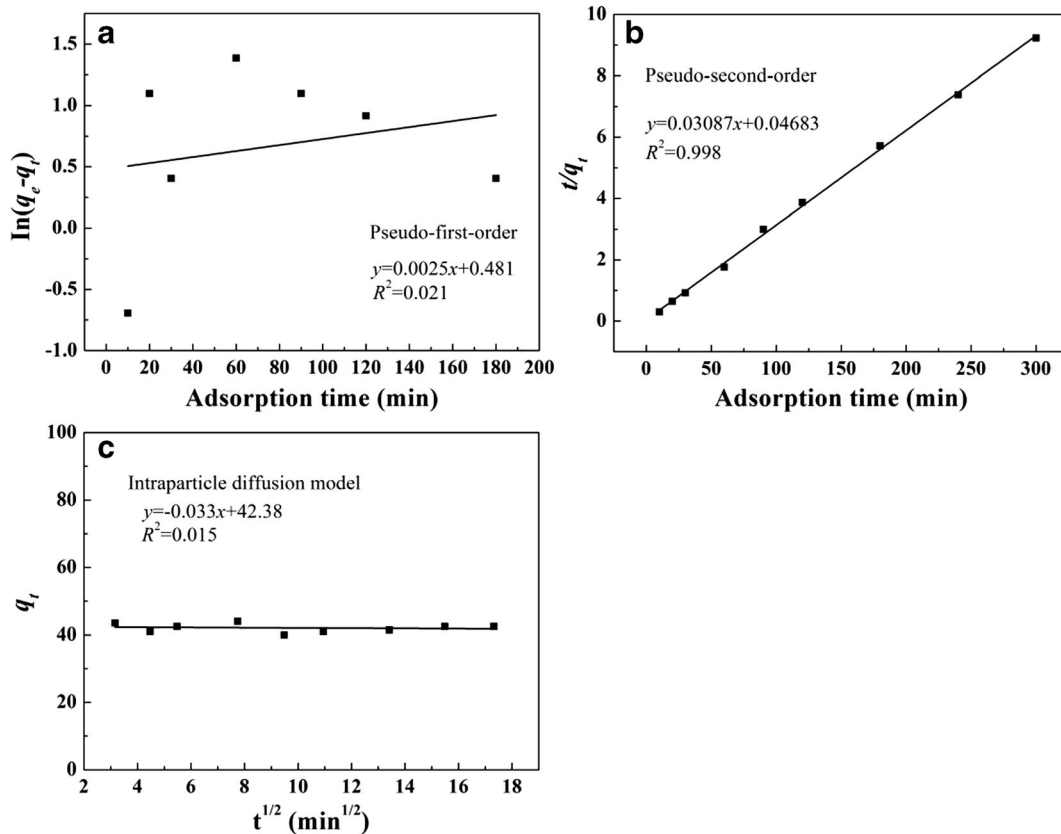


Fig. 9 Pseudo-first-order (a), pseudo-second-order (b), and intraparticle diffusion model (c) for Ag^+ adsorption onto the TCA-SNPs

textbook dealing with adsorption process (Abinashi et al. 2016; Ramakrishna et al. 2016). Figure 9 shows the goodness of the above models with the experimental data. The model parameters along with regression coefficients are listed in Table 3. Based on the goodness of the fit, the pseudo-second-order kinetic model is found to be appropriate to represent the rate of adsorption of Ag^+ ion using TCA-SNPs adsorbent.

Table 3 Kinetics parameters for Ag^+ adsorption on TCA-SNPs at 298 K

Kinetic models	Parameter	Value
Pseudo-first-order	K_1 (g/mg·min)	-0.0025
	R^2	0.021
Pseudo-second-order	K_2 (g/mg·min)	0.0203
	R^2	0.998
Intraparticle diffusion	K_i (mg/g·min ^{1/2})	-0.033
	C	42.38
	R^2	0.015

3.5 Adsorption-Desorption Cycle of TCA-SNPs

The adsorption isotherms clearly indicate superior performance of the TCA-SNPs as compared to other literature-reported adsorbent for the removal of Ag^+

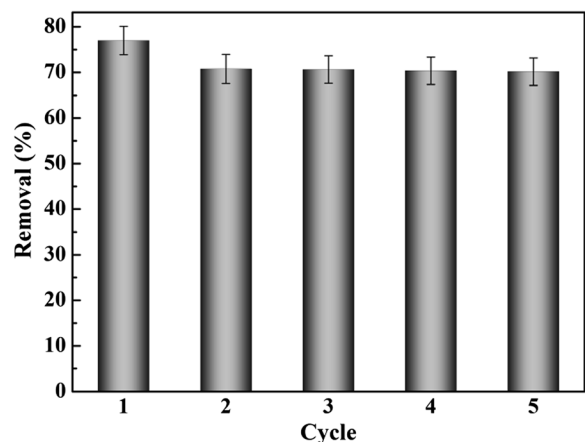


Fig. 10 Removal ratio of Ag^+ for TCA-SNPs after five consecutive cycles of desorption/adsorption

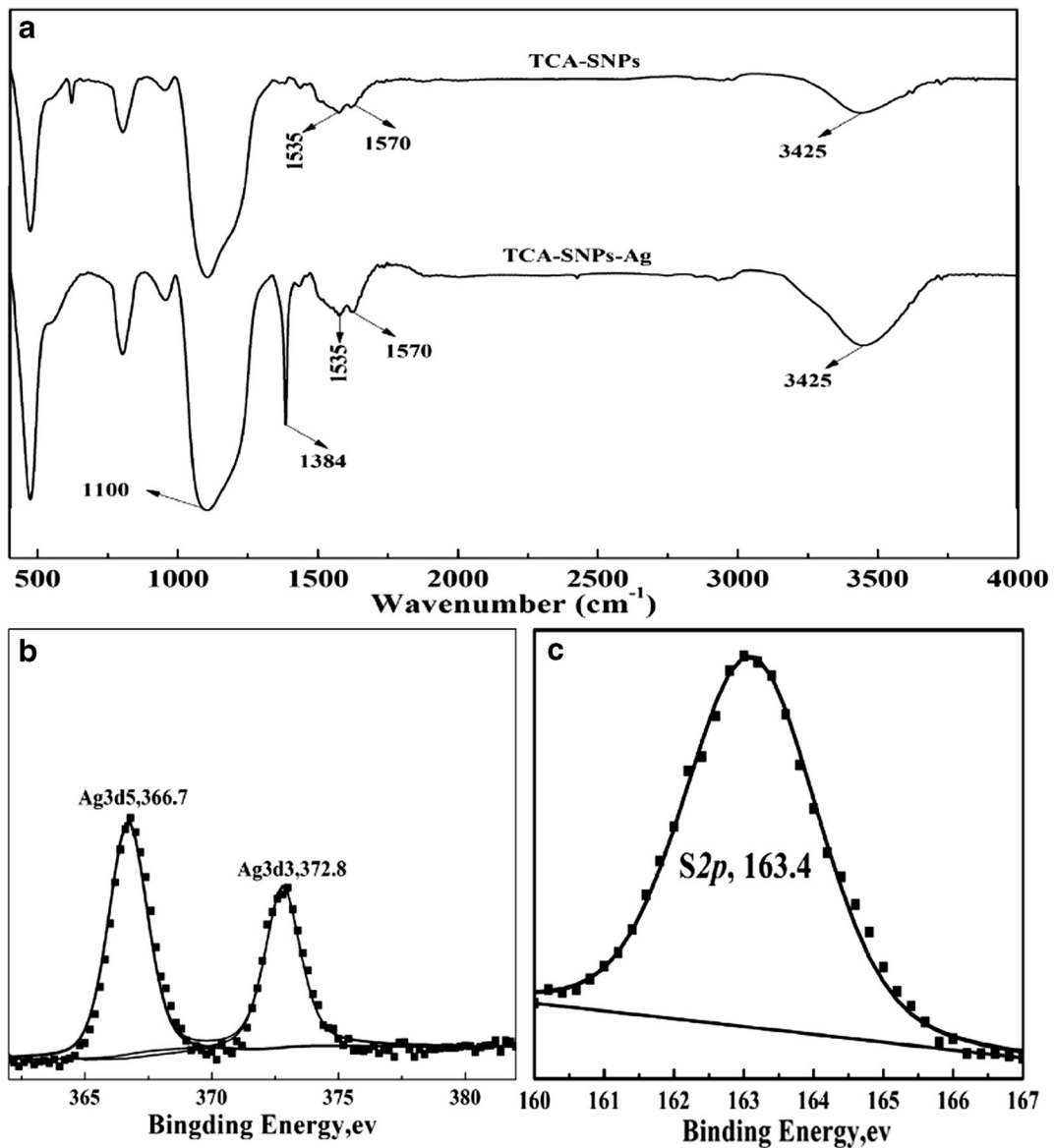


Fig. 11 FT-IR (a), XPS of Ag3d (b), and S2p (c) of TCA-SNPs-Ag

ion from liquid phase. However, the success of commercial adoption of an adsorbent additionally depends

on its ability to desorb and to be reused for many desorption/adsorption cycles. Hence to assess the ability

Table 4 Selective adsorption of TCA-SNPs for coexisting metal ions

Coexisting ions	Ag ⁺	Ag ⁺ +Mn ²⁺		Ag ⁺ +Cu ²⁺		Ag ⁺ +Ni ²⁺		Ag ⁺ +Co ³⁺	
		Ag ⁺	Mn ²⁺	Ag ⁺	Cu ²⁺	Ag ⁺	Ni ²⁺	Ag ⁺	Co ³⁺
C ₀ (mg/L)	100	100	25	100	25	100	25	100	25
C _e (mg/L)	25.2	19.3	24.8	20	24.9	22.3	24.6	24.3	24.8
q _e (mg/g)	37.4	40.5	0.10	40.0	0.05	38.9	0.20	37.9	0.10

to regenerate, the regeneration of the adsorbents was performed in a mixture of 10% thiourea and HNO_3 of concentration 1 mol/L. To test the reusability of adsorbent, adsorption tests were performed following the same procedure as reported earlier. Twenty milligrams of TCA-SNPs was added into 10 mL of silver ions solution, and then oscillated it for 5 h at pH 5 and room temperature. After that, TCA-SNPs adsorbent was desorbed for 5 h at room temperature using eluent (50 mL). Figure 10 shows performance of the TCA-SNPs adsorbent covering five consecutive desorption/adsorption cycles. A reduction in the removal ratio from 77.10 to 70.17% was observed for the first recycle run. The uncertainty of the removal ratio is 1.7%. However, subsequent cycles did not result in any significant reduction in the removal ratio, confirming the stability of the adsorbent to withstand number of desorption/adsorption cycles. The results clearly indicate good stability and high efficiency on repeated use.

3.6 Adsorption Mechanism of Silver Ions onto TCA-SNPs

In order to clarify the adsorption mechanism, Ag^+ loaded TCA-SNPs (defined as TCA-SNPs-Ag) were analyzed using FT-IR and XPS. After adsorption of Ag^+ , there is a strong adsorption peaks at 1384 cm^{-1} which came from nitrate ions attached to the adsorbent (Fig. 11a). The XPS of $\text{Ag}3d$ in TCA-SNPs-Ag is presented in Fig. 11b, the binding energy of $\text{Ag}3d$ around 366.7 and 372.8 eV in TCA-SNPs-Ag are significantly smaller than that in AgNO_3 (Tahmasebi and Yamini 2014), indicating higher the electron density at the Ag atoms than that of the free ligand. The peaks at 163.4 eV correspond to the sulfur bounding to Ag^+ (Fig. 11c) (Zhang et al. 2015; Bootharaju and Pradeep 2011). Moreover, the good reusability of adsorbent indicated that C-S bond is not broken. So, it is hardly possible to produce the Ag_2S compound. Thus, the results showed that the adsorption of TCA-SNPs for silver ions from an aqueous solution is based on coordination interactions between silver ions and thiol groups located on the surface of TCA-SNPs (Lu et al. 2010; Quang et al. 2013).

3.7 Effect of Coexisting Metal Ions

The presence of other metal ions such as Mn^{2+} , Cu^{2+} , Ni^{2+} , and Co^{3+} along with Ag^+ in industrial effluent is

common and hence it is necessary to assess the effect of these ions on the adsorption of Ag^+ on TCA-SNPs. Table 4 summarizes the effect of coexisting metal ions. It is clear from the C_e values reported in Table 4 the reduction in concentration of the other ions in comparison with the Ag^+ ion is insignificant. The results indicated that Ag^+ could be selectively separated from mixture solution.

4 Conclusions

We modified the surface of the silica nanoparticles with trithiocyanuric acid so as to enhance the adsorption of Ag^+ from aqueous solutions. The Ag^+ adsorption capacity increased with increase in the solution pH, with the optimal pH being 5. The maximal absorptive capacity of adsorbent TCA-SNPs on Ag^+ reached 80 mg/g at the optimal pH 5.0, significantly higher than the adsorption capacity reported for other adsorbents in literature. The increase in adsorption capacity was attributed to the coordination between Ag^+ and mercapto group on the surface of the modified adsorbents. The adsorption kinetics indicated very high rates of adsorption initially, with rapid reduction in rate of adsorption with time. The adsorption isotherm was found to match with the Langmuir model while the adsorption kinetics was found to match with the pseudo-second-order kinetic model. After used five times, the TCA-SNPs retained the higher regeneration efficiency ensuring commercial adoption. The TCA-SNPs had a relatively high adsorption of Ag^+ as compared to other ions such as Mn^{2+} , Cu^{2+} , Ni^{2+} , and Co^{3+} . In summary, the silica nanoparticles modified with trithiocyanuric acid have the potential application prospect to remove Ag^+ from aqueous solutions.

Acknowledgements The authors are grateful for the financial support from the National Natural Science Foundation (Nos. 51464024 and 51664037), the Yunnan Province Young Academic Technology Leader Reserve Talents (2012HB008), and the Yunnan Province Natural Science Foundation (2013FB096).

References

- Abinashi, S., Jeongwon, P., Hyoeun, K., & Pyung-Kyu, P. (2016). Arsenic removal from aqueous solutions by adsorption onto hydrous iron oxide-impregnated alginate beads. *Journal of Industrial and Engineering Chemistry*, 35, 277–286.

- Ali, L. I. A., Ibrahim, W. A. W., Sulaiman, A., Kamboh, M. A., & Sanagi, M. M. (2016). New chrysin-functionalized silica-core shell magnetic nanoparticles for the magnetic solid phase extraction of copper ions from water samples. *Talanta*, *148*, 191–199.
- Bootharaju, M. S., & Pradeep, T. (2011). Investigation into the reactivity of unsupported and supported Ag₇ and Ag₈ clusters with toxic metal ions. *Langmuir*, *27*, 8134–8143.
- Bose, P., Bose, M. A., & Kumar, S. (2002). Critical evaluation of treatment strategies involving adsorption and chelation for wastewater containing copper, zinc and cyanide. *Advances in Environmental Research*, *7*, 179–195.
- Cecen, F., Semerci, N., & Geyik, A. G. (2010). Inhibition of respiration and distribution of Cd, Pb, Hg, Ag and Cr species in a nitrifying sludge. *Journal of Hazardous Materials*, *178*, 619–627.
- Chang, Y. C., Chang, S. W., & Chen, D. H. (2006). Magnetic chitosan nanoparticles: studies on chitosan binding and adsorption of Co(II) ions. *Reactive and Functional Polymers*, *66*, 335–341.
- Coruh, S., Senel, G., & Ergun, O. N. (2010). A comparison of the properties of natural clinoptilolites and their ion-exchange capacities for silver removal. *Journal of Hazardous Materials*, *180*, 486–492.
- Eckelman, M. J., & Graedel, T. E. (2007). Silver emissions and their environmental impacts: a multilevel assessment. *Environmental Science & Technology*, *41*, 6283–6289.
- El-Shahawi, M. S., Bashammakh, A. S., & Bahaffi, S. O. (2007). Chemical speciation and recovery of gold(I, III) from wastewater and silver by liquid-liquid extraction with the ion-pair reagent amiloride mono hydrochloride and AAS determination. *Talanta*, *72*, 1494–1499.
- Ghaedi, M., Shokrollahi, A., Niknam, K., Niknam, E., Najibi, A., & Soylak, M. (2009). Cloud point extraction and flame atomic absorption spectrometric determination of cadmium(II), lead(II), palladium(II) and silver(I) in environmental samples. *Journal of Hazardous Materials*, *168*, 1022–1027.
- Hassan, M. L., & El-Wakil, N. A. (2003). Heavy metal ion removal by amidoximated bagasse. *Journal of Applied Polymer Science*, *87*, 666–670.
- He, C., Ren, L., Zhu, W., Xu, Y., & Qian, X. (2015). Removal of mercury from aqueous solution using mesoporous silica nanoparticles modified with polyamide receptor. *Journal of Colloid and Interface Science*, *458*, 229–234.
- Hou, H., Yu, D., & Hu, G. (2015). Preparation and properties of ion-imprinted hollow particles for the selective adsorption of silver ions. *Langmuir*, *31*, 1376–1384.
- Kirci, S., GÜlfen, M., & Aydin, A. O. (2009). Separation and recovery of silver(I) ions from base metal ions by thiourea-urea-formaldehyde chelating resin. *Separation Science and Technology*, *44*, 1869–1883.
- Li, X., Wang, Z., Li, Q., Ma, J., & Zhu, M. (2015). Preparation, characterization, and application of mesoporous silica-grafted graphene oxide for highly selective lead adsorption. *Chemical Engineering Journal*, *273*, 630–637.
- Lihareva, N., Dimova, L., Petrov, O., & Tzvetanova, Y. (2010). Ag⁺ sorption on natural and Na-exchanged clinoptilolite from Eastern Rhodopes. *Microporous and Mesoporous Materials*, *130*, 32–37.
- Liu, P., Borrell, P. F., Bozic, M., Kokol, V., Oksman, K., & Mathew, A. P. (2015). Nano-celluloses and their phosphorylated derivatives for selective adsorption of Ag⁺, Cu²⁺ and Fe³⁺ from industrial effluents. *Journal of Hazardous Materials*, *294*, 177–185.
- Lu, X., Yin, Q., Xin, Z., & Zhang, Z. (2010). Powerful adsorption of silver(I) onto thiol-functionalized polysilsesquioxane microspheres. *Chemical Engineering Science*, *65*, 6471–6477.
- Manzoori, J. L., Abdolmohammad-Zadeh, H., & Amjadi, M. (2007). Ultra-trace determination of silver in water samples by electrothermal atomic absorption spectrometry after preconcentration with a ligand-less cloud point extraction methodology. *Journal of Hazardous Materials*, *144*, 458–463.
- Manzoori, J. L., Amjadi, M., & Hallaj, T. (2009). Preconcentration of trace cadmium and manganese using 1-(2-pyridylazo)-2-naphthol-modified TiO₂ nanoparticles and their determination by flame atomic absorption spectrometry. *International Journal of Environmental Analytical Chemistry*, *89*, 749–758.
- Monier, M., Ayad, D. M., & Sarhan, A. A. (2010). Adsorption of Cu(II), Hg(II) and Ni(II) ions by modified natural wool chelating fibers. *Journal of Hazardous Materials*, *176*, 348–355.
- Moshhadizadeh, M. H., & Karami, Z. (2011). Solid phase extraction of trace amounts of Ag, Cd, Cu, and Zn in environmental samples using magnetic nanoparticles coated by 3-(trimethoxysilyl)-1-propanol and modified with 2-amino-5-mercapto-1,3,4-thiadiazole and their determination by ICP-OES. *Journal of Hazardous Materials*, *190*, 1023–1029.
- Nguyen-Phan, T. D., Pham, H. D., Kim, S., Oh, E. S., Kim, E. J., & Shin, E. W. (2010). Surfactant removal from mesoporous TiO₂ nanocrystals by supercritical CO₂ fluid extraction. *Journal of Industrial and Engineering Chemistry*, *16*, 823–828.
- Peng, X., Zhang, W., Gai, L., Jiang, H., Wang, Y., & Zhao, L. (2015). Dedoped Fe₃O₄/PPy nanocomposite with high anti-interfering ability for effective separation of Ag(I) from mixed metal-ion solution. *Chemical Engineering Journal*, *280*, 197–205.
- Pourreza, N., Rastegarzadeh, S., & Larki, A. (2014). Nano-TiO₂ modified with 2-mercaptobenzimidazole as an efficient adsorbent for removal of Ag(I) from aqueous solutions. *Journal of Industrial and Engineering Chemistry*, *20*, 127–132.
- Quang, D. V., Lee, J. E., Kim, J., Kim, Y. N., Shao, G. N., & Kim, H. T. (2013). A gentle method to graft thiol-functional groups onto silica gel for adsorption of silver ions and immobilization of silver nanoparticles. *Powder Technology*, *235*, 221–227.
- Reddy, S. R., Pandey, N. K., Mallika, C., & Mudali, U. K. (2016). Equilibrium and kinetics of adsorption of ruthenium on activated charcoal from nitric acid solutions. *Chemical Engineering Research and Design*, *115*, 91–97.
- Saif, A. C., Zakiullah, Z., & Sharf, I. S. (2017). Isotherm, kinetic and thermodynamics of arsenic adsorption onto iron-zirconium binary oxide-coated sand (IZBOCS): modelling and process optimization. *Molecular Liquids*, *229*, 230–240.
- Shin, K. Y., Hong, J. Y., & Jang, J. (2011). Heavy metal ion adsorption behavior in nitrogen-doped magnetic carbon nanoparticles: isotherms and kinetic study. *Journal of Hazardous Materials*, *190*, 36–44.

- Soumya, R. M., Rachna, C., Jipsi, K. A., & Savariya, D. B. (2017). Kinetics and isotherm studies for the adsorption of metal ions onto two soil types. *Environmental Technology & Innovation*, 7, 87–101.
- Soylak, M., Cay, R. S. (2007). Separation/preconcentration of silver(I) and lead(II) in environmental samples on cellulose nitrate membrane filter prior to their flame atomic absorption spectrometric determinations. *Journal of Hazardous Materials*, 146, 142–147.
- Tahmasebi, E., & Yamini, Y. (2014). Polythiophene-coated Fe₃O₄ nanoparticles as a selective adsorbent for magnetic solid-phase extraction of silver(I), gold(III), copper(II) and palladium(II). *Microchimica Acta*, 181, 543–551.
- Tang, B., Yu, G., Fang, J., & Shi, T. (2010). Recovery of high-purity silver directly from dilute effluents by an emulsion liquid membrane-crystallization process. *Journal of Hazardous Materials*, 177, 377–383.
- Xie, F., Lin, X., Wu, X., & Xie, Z. (2008). Solid phase extraction of lead(II), copper(II), cadmium(II) and nickel(II) using gallic acid-modified silica gel prior to determination by flame atomic absorption spectrometry. *Talanta*, 74, 836–843.
- Yirikoglu, H., & GÜlfen, M. (2008). Separation and recovery of silver(I) ions from base metal ions by melamine-formaldehyde-thiourea (MFT) chelating resin. *Separation Science and Technology*, 43, 376–388.
- Zeliyha, Ç., Gülfen, M., & Aydın, A. O. (2010). Synthesis of a novel dithioxamide-formaldehyde resin and its application to the adsorption and separation of silver ions. *Journal of Hazardous Materials*, 174, 556–562.
- Zhang, S. W., Xu, W. Q., Zeng, M. Y., Li, J., Li, J. X., Xu, J. Z., & Wang, X. K. (2013). Superior adsorption capacity of hierarchical iron oxide@magnesium silicate magnetic nanorods for fast removal of organic pollutants from aqueous solution. *Journal of Materials Chemistry A*, 1, 11691–11697.
- Zhang, M., Zhang, Y., & Helleur, R. (2015). Selective adsorption of Ag⁺ by ion-imprinted O-carboxymethyl chitosan beads grafted with thiourea-glutaraldehyde. *Chemical Engineering Journal*, 264, 56–65.
- Zhang, S. W., Fan, Q. H., Gao, H. H., Huang, Y. S., Liu, X., Li, J. X., Xu, X. J., & Wang, X. K. (2016). Formation of Fe₃O₄@MnO₂ ball-in-ball hollow spheres as a high performance catalyst with enhanced catalytic performances. *Journal of Materials Chemistry A*, 4, 1414–1422.
- Zhang, L. B., Zhang, G. W., Wang, S. X., Peng, J. H., & Cui, W. (2017). Sulfoethyl functionalized silica nanoparticle as an adsorbent to selectively adsorb silver ions from aqueous solutions. *Journal of the Taiwan Institute of Chemical Engineers*, 71, 330–337.
- Zhao, Y. G., Li, J. X., Zhang, S. W., & Wang, X. K. (2014a). Amidoxime-functionalized magnetic mesoporous silica for selective sorption of U(VI). *RSC Advances*, 4, 32710–32717.
- Zhao, Y. G., Li, J. X., Zhao, L. P., Zhang, S. W., Huang, Y. S., Wu, X. L., & Wang, X. K. (2014b). Synthesis of amidoxime-functionalized Fe₃O₄@SiO₂ core-shell magnetic microspheres for highly efficient sorption of U(VI). *Chemical Engineering Journal*, 235, 275–283.
- Zhao, Y. G., Wang, X. X., Li, J. X., & Wang, X. K. (2015). Amidoxime functionalization of mesoporous silica and its high removal of U(VI). *Polymer Chemistry*, 6, 5376–5384.